Cationic Ring-Opening Copolymerization of Cyclic Acetals and 1,3-Dioxolan-4-ones via the Activated Monomer Mechanism and Transacetalization Reaction

Kana Takebayashi, Arihiro Kanazawa, and Sadahito Aoshima**

Department of Macromolecular Science, Graduate School of Science, Osaka University, Toyonaka, Osaka 560-0043, Japan.

For TOC Use Only

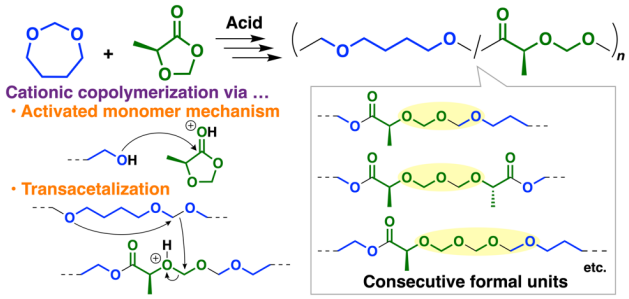

Abstract

Cationic ring-opening copolymerization of cyclic acetals and 1,3-dioxolan-4-ones (DOLOs) was examined with a particular focus on elucidating the polymerization mechanisms. Cationic copolymerization of 1,3-dioxepane and 5-methyl-1,3-dioxolan-4-one successfully proceeded with CF_3SO_3H as a protonic acid catalyst, yielding copolymers. The main portion of these copolymers exhibited number-average molecular weight values greater than 10^4 (determined except for oligomer peaks). Detailed structural analyses of the copolymers were performed by NMR spectrometry and electrospray ionization mass spectrometry. The result suggested that copolymerization occurs via an activated monomer mechanism involving the reaction of a hydroxy group and a proton-attached DOLO. In addition, acid-catalyzed transacetalization reactions with hemiformal chain ends and formal moieties most likely occurred during copolymerization, resulting in consecutive formal structures in the main chain.

Introduction

Cationic ring-opening copolymerizations between different types of cyclic monomers, such as cyclic ethers, cyclic esters, and cyclic acetals, exert great potential, particularly in controlling monomer sequences, tuning the physical properties of polymers, providing copolymers with degradability, and overcoming inertness, such as nonhomopolymerizability.[1–10] The features attained by copolymerization rather than homopolymerization are ascribed to various possible reactions, such as propagation, backbiting, and transacetalization reactions, that occur during cationic ring-opening polymerization. In addition, two main types of propagation mechanisms may occur in cationic ring-opening polymerization. One is the active chain end (ACE) mechanism,[11,12] as in the reaction of a cyclic ether-derived oxonium ion with a cyclic ether monomer, and the other is the activated monomer (AM) mechanism,[13–16] as exemplified by the reaction of a hydroxy chain end with a proton-activated cyclic ester monomer. Interestingly, even when a common monomer is used in copolymerizations, the propagation mechanisms differ depending on the reaction conditions and the types of comonomers.

Our group recently examined the cationic copolymerization of cyclic acetals (such as 2-methyl-1,3-dioxepane) and cyclic esters (such as ε-caprolactone and δ-valerolactone) using $EtSO_3H$ as a protonic acid catalyst, and we determined that the reaction proceeds via mechanisms involving the AM mechanism and transacetalization (Scheme 1A).[17,18] In addition, monomer sequences of copolymers from multiblock sequences containing isolated cyclic ester units can be transformed into alternating sequences through controlling the transacetalization reactions and polymerization–depolymerization equilibrium, which is achieved by vacuuming or a temperature change. Basko and coworkers reported the cationic copolymerization of 1,3-dioxolane and lactide using CF_3SO_3H as a catalyst.[19] The AM mechanism was suggested to occur when using an alcohol initiator.

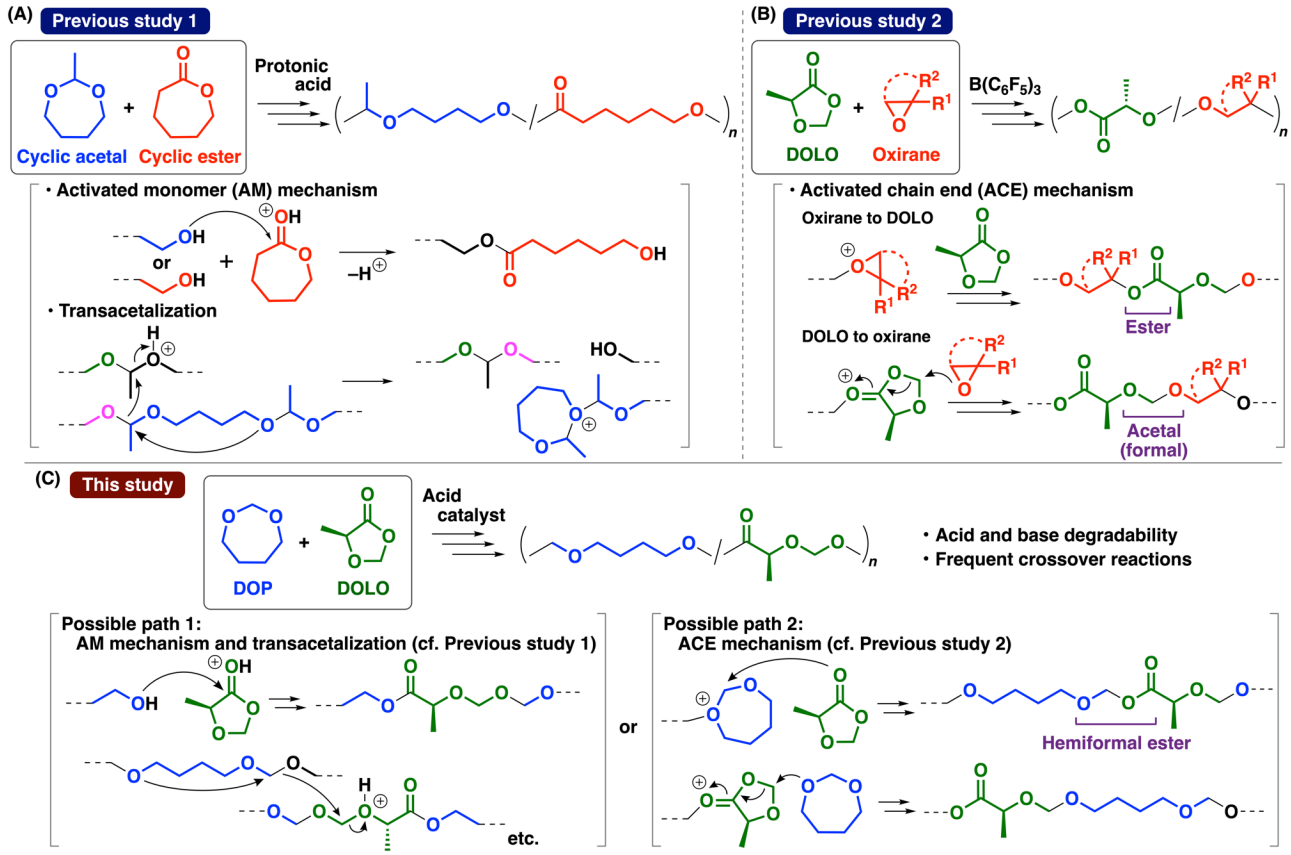

Scheme 1. Cationic Copolymerizations of (A) Cyclic Acetal and Cyclic Ester (2-Methyl-1,3-Dioxepane and ε-Caprolactone as Examples); (B) DOLO (5-Methyl-1,3-dioxolan-4-one as an Example) and Oxirane; and (C) Cyclic Acetal and DOLO (1,3-Dioxepane and 5-Methyl-1,3-dioxolan-4-one as Examples).

Unlike the above examples involving the AM mechanism, the cationic copolymerization of oxiranes, such as isobutylene oxide and 4-vinyl-1-cyclohexene-1,2-epoxide, and 1,3-dioxolan-4-ones (DOLOs) proceeds via the ACE mechanism using $B(C_6F_5)_3$ as a Lewis acid catalyst, as reported in our previous study.[20] The oxirane-derived oxonium ion reacts with the carbonyl group of DOLOs and leads to subsequent ring-opening via the reaction with an oxirane (Scheme 1B). A carbocation can also be generated via the ring-opening of the DOLO-derived oxonium ion. Terpolymerization of vinyl ether, oxirane, and DOLO was also possible via reactions involving the crossover reaction from the DOLO-derived carbocation to a vinyl ether. DOLOs[21–24] were reported to homopolymerize via the elimination of carbonyl compounds by the coordination–insertion ring-opening polymerization using a metal catalyst;[24] however, DOLOs are cationically nonhomopolymerizable,[20] unlike six- or seven-membered cyclic hemiacetal esters[25,26] and bicyclic cyclic hemiacetal esters.[27] Therefore, utilizing

oxiranes as comonomers is of great importance for enabling the cationic polymerization of DOLOs.

On the basis of this background, we were interested in the cationic copolymerization of cyclic acetals and DOLOs (Scheme 1C) because these monomers potentially undergo various reactions, such as propagation by the ACE mechanism, propagation by the AM mechanism, transacetalization, polymerization–depolymerization equilibrium, and carbocation generation. In this study, we examined the cationic copolymerizations of the cyclic acetals and DOLOs listed in Scheme 2 using Lewis acids or protonic acids as catalysts. As a result, copolymerizations of suitable monomer pairs successfully proceeded with a strong protonic acid, yielding copolymer products. The main portion of these copolymers exhibited number-average molecular weight (M_n) values greater than 10^4. Considering the above copolymerization examples (Scheme 1A and 1B), the copolymerization of cyclic acetals and DOLOs was expected to proceed via either the AM mechanism (Scheme 1C, left) or the ACE mechanism (Scheme 1C, right). Structural analysis of the product obtained from 1,3-dioxepane (DOP) and 5-methyl-1,3-dioxolan-4-one (**1**) by NMR and electrospray ionization mass spectrometry (ESI-MS) revealed that copolymerization occurred via the AM mechanism and transacetalization. In addition, the copolymers were degradable via cleavage of the formal (–O–CH_2–O–) and ester moieties in the main chain.

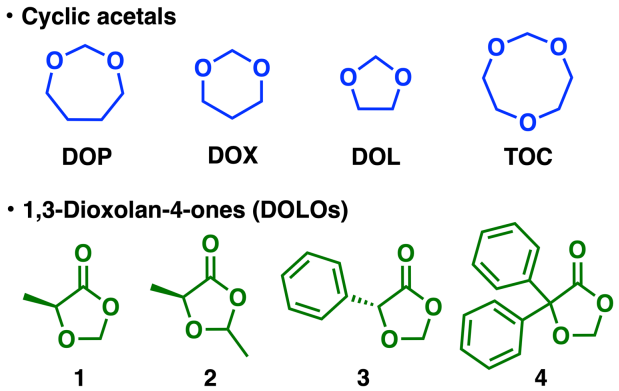

Scheme 2. Monomers Used in This Study.

Experimental Section

See the Supporting Information for the Materials, Characterization, and Transacetalization subsections.

Polymerization. An example of the copolymerization of DOP and **1** with CF_3SO_3H is described as follows. A glass tube equipped with a three-way stopcock was dried using a heat gun (Ishizaki PJ-206A; the blowing temperature was approximately 450 °C) under a dry nitrogen atmosphere. Dichloromethane, hexane (as an internal standard), DOP, and **1** were sequentially added to the tube using dry syringes. Polymerization was initiated by adding a CF_3SO_3H solution in dichloromethane at room temperature (25 °C). After predetermined intervals, aliquots were withdrawn from the reaction solution using dry syringes and subsequently added to vials containing methanol and a small amount (approximately 1%) of aqueous ammonia (reaction solution/methanol solution: 1/1 to 2/1 v/v). The quenched mixtures were diluted with dichloromethane and washed with water. The volatiles were removed under reduced pressure at 50 °C to afford polymers. Monomer conversion was calculated from ^{1}H NMR of the quenched reaction mixture; gas chromatography (GC) analysis and ^{1}H NMR of the purified polymer; or GC analysis.

Transesterification. A polymer was dissolved in butyl acetate. Transesterification was started by adding a $Ti(OBu)_4$ solution. After the reaction was performed at 70 °C for 19 h, the solution was diluted with dichloromethane at room temperature to quench the reaction. The quenched solution was washed with water, and volatiles were removed under reduced pressure at 60 °C to yield a product.

Results and Discussion

Cationic Copolymerization of DOP and 1

Cationic copolymerization was examined using DOP and **1** as monomers with various acids to construct suitable reaction conditions. When $B(C_6F_5)_3$ was used as a catalyst at –78 °C, which are

suitable conditions for the cationic copolymerization of oxiranes and DOLOs (Scheme 1B),[20] polymer or oligomer products were not obtained (entry 1 in Table 1). The reaction using $B(C_6F_5)_3$ at 25 °C was also not effective (entry 2). Oligomers were obtained when $GaCl_3$ or $SnCl_4$ was used; however, the amounts of incorporated **1** were obviously small (entries 3 and 4). Unlike the reactions using Lewis acid catalysts, the copolymerization using $PhSO_3H$ resulted in polymers with both M_n values higher than 10^3 and adequate amounts of **1** units (entries 5 and 6; Figure 1A and B). Most of the products obtained by the copolymerization of DOP and **1** exhibited bimodal molecular weight distributions (MWDs) consisting of a large peak in the high-molecular-weight (high-MW) region and a small peak in the low-MW region; hence, two M_n values that correspond to a main peak and whole peaks were determined for each sample below. Dichloromethane (entry 6; $M_n = 11 \times 10^3$ for a main peak) was superior to toluene (entry 5; $M_n = 4.2 \times 10^3$ for a main peak) in terms of MWs, which was corroborated by the occurrence of Friedel–Crafts reactions with toluene and propagating carbocations (Figure S1). Polymerization was faster in toluene than in dichloromethane although the reason of the faster polymerization in the less polar solvent is currently unclear.

Table 1. Cationic Homopolymerization of **1** and Copolymerization of Cyclic Acetals and **1**.[a]

entry	cyclic acetal	conc (M)		catalyst	solvent	time	conv (%)[b]		$M_n \times 10^{-3}$ [c]	M_w/M_n [c]	unit ratios[d]
		acetal	**1**				acetal	**1**			acetal/**1**
1	DOP	1.5	1.5	$B(C_6F_5)_3$	CH_2Cl_2	119 h	6	4	–	–	–
2	DOP	0.75	0.75	$B(C_6F_5)_3$	toluene	436 h	8	2	–	–	–
3	DOP	0.75	0.75	$GaCl_3$	toluene	94 h	50	10	0.8	2.83	23/1.0 (96%/4%)
4	DOP	0.75	0.75	$SnCl_4$	toluene	94 h	24	<1	0.7	2.56	65/1.0 (98%/2%)
5	DOP	1.5	1.5	$PhSO_3H$	toluene	115 h	100	69	1.9 (4.2)[e]	3.55	1.8/1.0 (64%/36%)
6	DOP	1.5	1.5	$PhSO_3H$	CH_2Cl_2	167 h	40	9	2.4 (11)[e]	7.82	4.6/1.0 (82%/18%)
7	DOP	1.5	1.5	CF_3SO_3H	CH_2Cl_2	118 h	76	36	4.2 (15)[e]	5.96	2.1/1.0 (68%/32%)
						269 h	83	48	4.1 (15)[e]	6.87	1.7/1.0 (63%/37%)
8	DOP	3.0	3.0	CF_3SO_3H	CH_2Cl_2	141 h	91	37	5.7 (15)[e]	4.77	2.5/1.0 (71%/29%)
9	DOP	1.5	3.0	CF_3SO_3H	CH_2Cl_2	167 h	45	39	4.3 (11)[e]	4.64	1.2/1.0 (55%/45%)
10	None	–	3.0	CF_3SO_3H	CH_2Cl_2	168 h	–	6[f]	–	–	–
11	DOX	1.5	1.5	CF_3SO_3H	CH_2Cl_2	119 h	0	0	–	–	–
12	DOL	1.5	1.5	CF_3SO_3H	CH_2Cl_2	119 h	49	39	1.1 (3.1)[e]	3.37	1.3/1.0 (57%/43%)
13	TOC	1.5	1.5	CF_3SO_3H	CH_2Cl_2	69 h	93	21	2.6 (7.5)[e]	5.76	4.5/1.0 (82%/18%)

[a] $[Catalyst]_0 = 4.0$ (entries 1, 2 and 5–13) or 5.0 (entries 3 and 4) mM at 25 (room temperature; entries 2–7), 30 (entries 8–13), or –78 (entry 1) ºC. [b] Calculated from ^1H NMR of the quenched reaction

mixture (entries 1–4 and 11); GC analysis and ^{1}H NMR of the purified polymer (entries 5–9, 12, and 13); or GC analysis (entry 10). [c] By GPC (polystyrene calibration). [d] Calculated by ^{1}H NMR. [e] Values for a main peak (a polymer peak). Oligomer peaks were not used for calculation of M_n. [f] A polymer product was not obtained. The conversion value (6%) includes an experimental error.

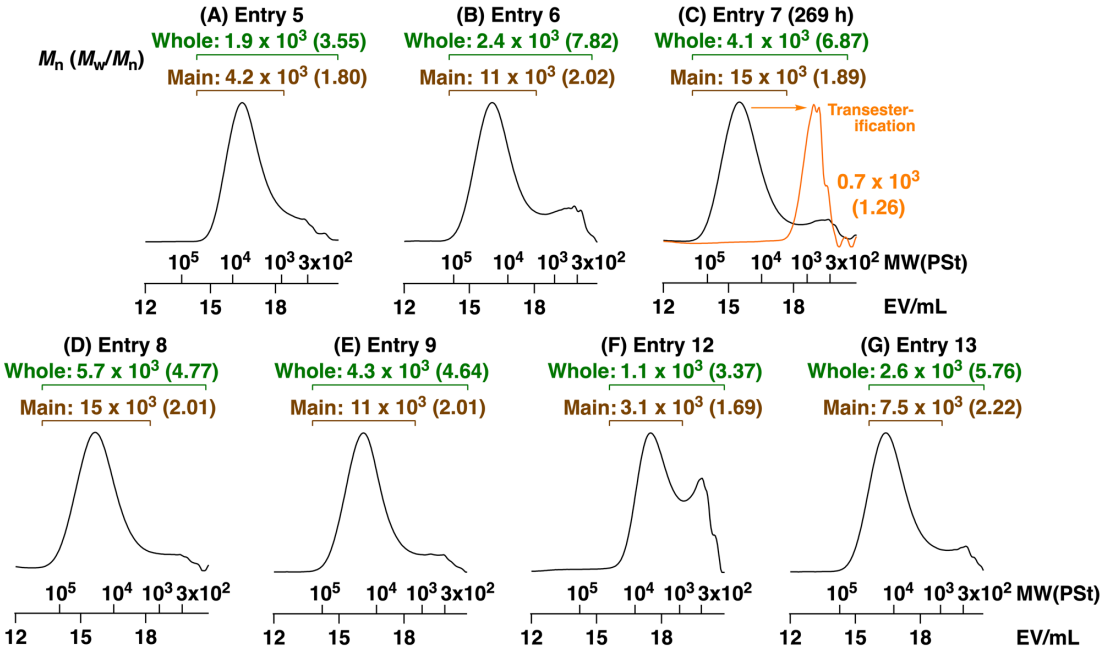

Figure 1. MWD curves of the polymers listed in Table 1: (A) entry 5, (B) entry 6, (C) entry 7 (269 h), (D) entry 8, (E) entry 9, (F) entry 12, and (entry 13) (orange curve of (C): transesterification product, 25 mM $Ti(OBu)_4$ in butyl acetate/dichloromethane (8/1 v/v; 0.3 wt% polymer) at 70 ºC for 19 h). See the footnote of Table 1 for the polymerization conditions.

Compared to the $PhSO_3H$ cases, the copolymerization using CF_3SO_3H as a protonic acid was demonstrated to attain higher monomer conversion and polymers with higher MWs. Polymers obtained by the copolymerization of DOP and **1** with CF_3SO_3H in dichloromethane at 25 °C exhibited a large peak in the higher-MW region and a small peak in the lower-MW region of the MWD curves (entry 7 in Table 1; Figure 1C). The M_n values calculated based on the whole region including oligomer peaks were 4.2×10^3 (118 h) and 4.1×10^3 (269 h); however, the M_n values calculated from the main peak (polymer peak) were approximately 15×10^3, which was obviously higher than the M_n values of the products obtained by $PhSO_3H$ (entries 5 and 6; vide supra). A similar polymer was obtained at higher concentrations of monomers (entry 8; Figure 1D).

^{1}H NMR analysis of the obtained polymer suggested that DOP and **1** were incorporated into

polymer chains (Figure 2A). Peaks at 1.6 ppm (peaks *c*, *c′*, *c*") and 3.6 ppm (peaks *b*, *b′*, *b″*) were assignable to the methylene groups of DOP units, while a peak at 1.4 ppm (*g*) was assigned to the methyl group of **1** units. In contrast to the spectrum of a DOP homopolymer, in which a single peak was observed at 4.7 ppm (peak *a*) (Figure 2B), many peaks were observed at 4.6–5.0 ppm (peaks *a*, *h*, *h′*, *h″*), which were assigned to various formal (–O–CH_2–O–) structures positioned in different environments. Peaks *h*, *h′*, and *h″* are assignable to isolated formal moieties adjacent to a **1** unit, formal moieties adjacent to formal and oxybutylene units, and formal moieties bearing **1** units and/or formal units at both sides, respectively. Notably, peaks were not observed at 5.0–5.5 ppm. Thus, a hemiformal ester structure (peak *i*), which potentially results from the crossover reaction from the DOP-derived cation to **1**, as occurred in the copolymerization of oxiranes and DOLOs (Scheme 1B), is negligible in the product from DOP and **1**.

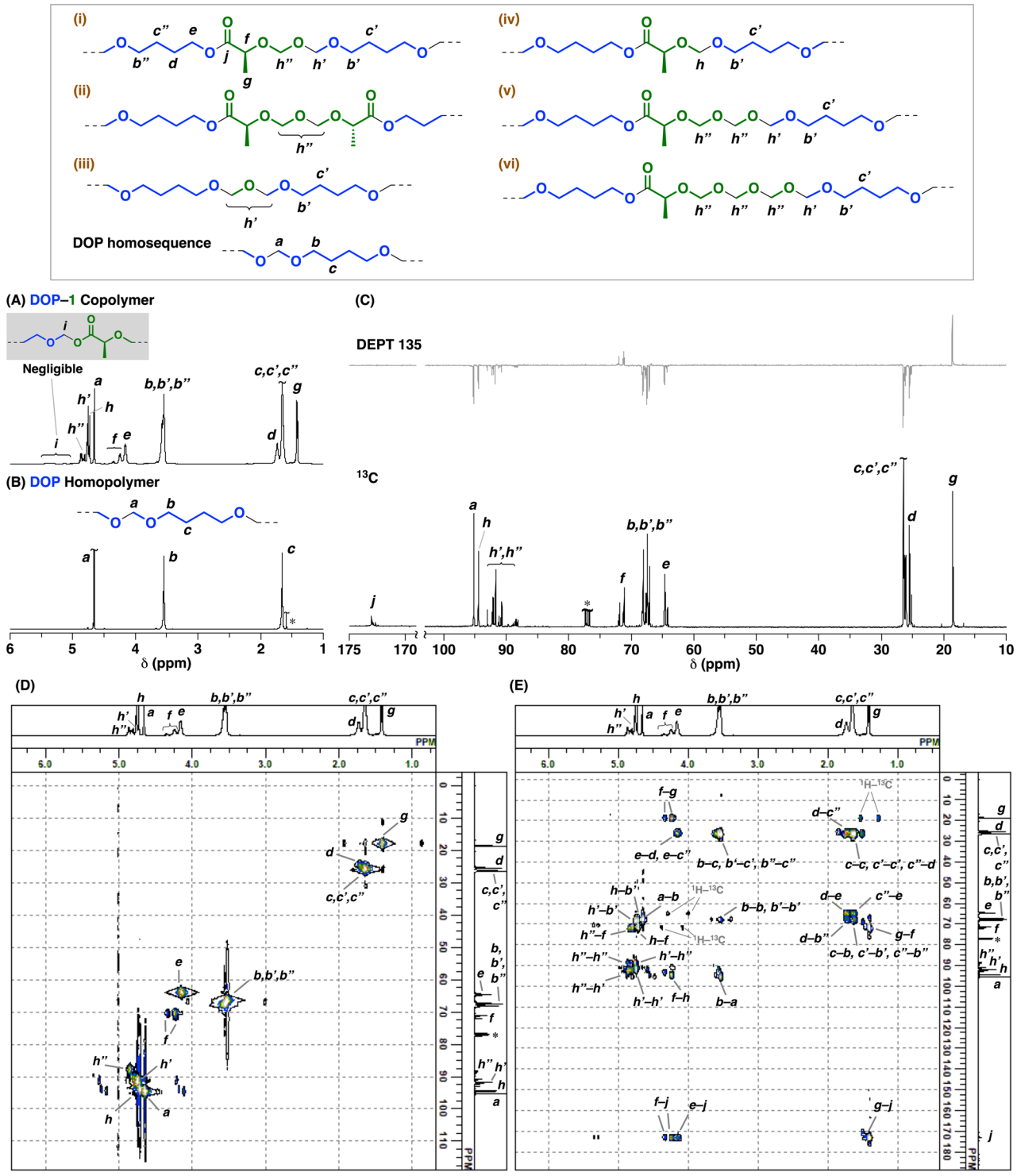

Figure 2. (A) ^{1}H; (C) ^{13}C and DEPT 135; (D) ^{1}H–^{13}C HSQC; and (E) ^{1}H–^{13}C HMBC NMR spectra of poly(DOP-*co*-**1**) (a polymer obtained under the same conditions as those for entry 7 in Table 1 and Figure 1C; M_n(GPC) = 4.0 × 10^3 (main: 14 × 10^3), M_w/M_n(GPC) = 7.28 (main: 2.07)). (B) ^{1}H NMR spectrum of poly(DOP) ([DOP]$_0$ = 3.0 M, [CF_3SO_3H]$_0$ = 4.0 mM, in CH_2Cl_2; M_n(GPC) = 6.3 × 10^3, M_w/M_n(GPC) = 8.10). * Water, $CHCl_3$, or $CDCl_3$. In $CDCl_3$ at 30 ºC.

To investigate the polymer structures in more detail, ^{13}C, DEPT 135, ^{1}H–^{1}H COSY, ^{1}H–^{13}C HSQC, and ^{1}H–^{13}C HMBC NMR spectra of the product were analyzed with a particular focus on the

formal structures (Figures 2 and S2; diffusion-ordered NMR spectroscopy (DOSY)[28,29] was also conducted (Figure S3)). In the ^{13}C NMR spectrum (Figure 2C), many methylene carbon peaks assignable to formal structures were observed at 88–96 ppm (peaks *a*, *h*, *h′*, *h″*). Correlations were confirmed between the peaks at 4.6–5.0 ppm in the ^{1}H NMR spectrum and the peaks at 88–96 ppm in the ^{13}C NMR spectrum in the ^{1}H–^{13}C HSQC spectrum (Figure 2D), confirming the assignments of these peaks to formal structures. Interestingly, correlations between these ^{1}H and ^{13}C NMR peaks were also observed in the ^{1}H–^{13}C HMBC NMR spectrum (Figure 2E; labeled *h′*–*h″*). Therefore, formal structures that are consecutively connected but not isolated most likely occurred, as exemplified by structures i, ii, iii, v, and vi in Figure 2. In addition, the assignments of peaks *h*, *h′*, and *h″* are consistent with the correlations observed in the ^{1}H–^{13}C HMBC NMR spectrum. Different chemical shifts of consecutive formal protons (4.6–5.0 ppm) and carbons (88–96 ppm) correspond to the study on compounds consisting of one to four consecutive formal units.[30] Other structures, such as the ester oxygen-adjacent methylene (peak *e*), the DOLO-derived methine (peak *f*), and the DOLO-derived carbonyl carbon (peak *j*), were also reasonably assigned to peaks in the NMR spectra.

Consecutive formal structures were also confirmed by ESI-MS analysis of the product obtained by the copolymerization of DOP and **1** (Figure 3). Peaks with *m*/*z* values consistent with structures composed of DOP units, **1** units, and oxymethylene units were detected. For example, the peak labeled with "[cyclic] $n + m = 10$, OM = 2" in Figure 3 corresponds to a total of 10 units of DOP and **1** (these monomers exhibit very similar molar masses (102.1; $C_5H_{10}O_2$ for DOP and $C_4H_6O_3$ for **1**)) and two oxymethylene units. Thus, consecutive formal structures consisting of several oxymethylene units occurred in the main chain. Polymer chains from which oxymethylene units were removed were also present, as demonstrated by the detection of peaks such as that labeled with "[cyclic] $n + m = 11$, OM = –2". This suggests that consecutive formal units were likely generated by the reactions between oxymethylene units in different polymer chains. In addition, the polymer chains corresponding to these peaks probably exhibit cyclic structures (see below for the possible mechanism

of cyclization) because the mass values are consistent with the sum of the molar masses of monomers and oxymethylene units. Linear chains that have water-derived chain ends are likely present as well (e.g., the peak labeled with "[H,OH] $n + m = 10$, OM = 0").

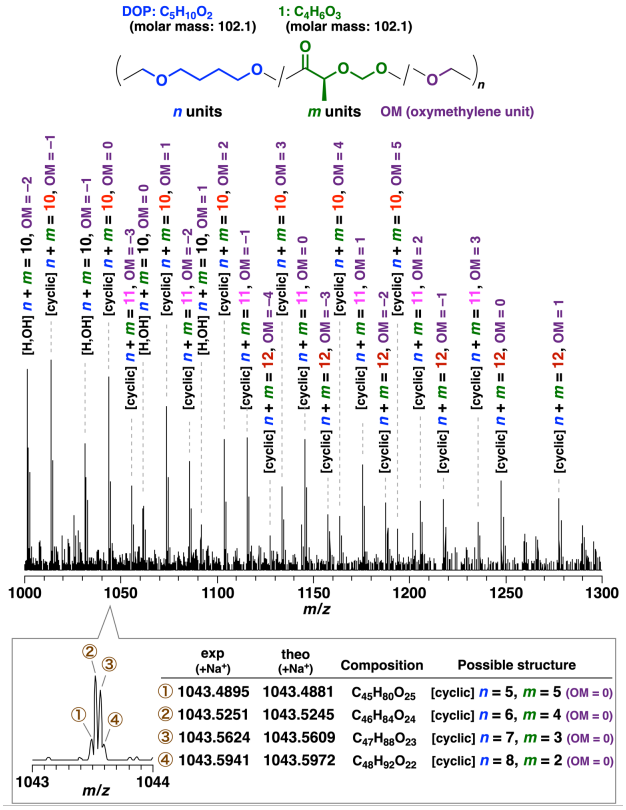

Figure 3. ESI-MS analysis (recorded by equipment with the Kingdon trap) of the product obtained by the copolymerization of DOP and **1** ($[DOP]_0 = 0.75$ M, $[\mathbf{1}]_0 = 0.75$ M, $[CF_3SO_3H]_0 = 4.0$ mM, in toluene at 25 ºC; M_n(GPC) = 1.5 × 10^3, M_w/M_n(GPC) = 3.26). The label [cyclic] means that the *m*/*z* values agreed with cyclic chains. The label [H,OH] means that the *m*/*z* values agreed with linear chains with H (a proton derived from adventitious water or the acid catalyst) and OH (derived from adventitious water) moieties at chain ends.

Degradation of Poly(DOP-*co*-1) by Transesterification and Transacetalization

To further confirm the copolymer structures, a transesterification reaction (Figure 4A) was conducted. The copolymer shown in Figure 1C (entry 7 in Table 1) was reacted with butyl acetate using $Ti(OBu)_4$ as a catalyst. After the reaction for 19 h, a low-MW product (M_n = 0.7 × 10^3) was obtained (the orange curve in Figure 1C; see Figure S3 for the ^{1}H NMR spectrum). ESI-MS analysis (Figure 4B) revealed that products derived from the possible copolymer structures shown in Figure 2

were obtained by transesterification. Specifically, the *m*/*z* values of the peaks agreed with the masses of products consisting of one **1** unit, one or more DOP units, a butoxy unit, and an acetoxy unit (X); and the masses of products consisting of two **1** units, zero or more DOP units, a methylene unit, and two butoxy units (Y). Importantly, peaks assignable to structures X and Y with additional oxymethylene units were also observed, which is consistent with the ESI-MS spectrum of the copolymer (vide supra; Figure 3). For example, a structure assigned to the peak labeled "X n = 1, OM = 1" in Figure 4B consists of one **1** unit, one DOP unit, a butoxy unit, an acetoxy unit, and an oxymethylene unit. These products support the presence of consecutive formal units in the original copolymer. Peaks assignable to structures with deficient oxymethylene units (e.g., a peak labeled with "X n = 1, OM = –1") were also detected, as observed for the copolymer (Figure 3). In addition, peaks assigned to structures containing one, two, and three DOP units (n or $n + n'$ = 1, 2, and 3) were mainly observed, which indicates that the original copolymer has short randomly distributed DOP homosequences.

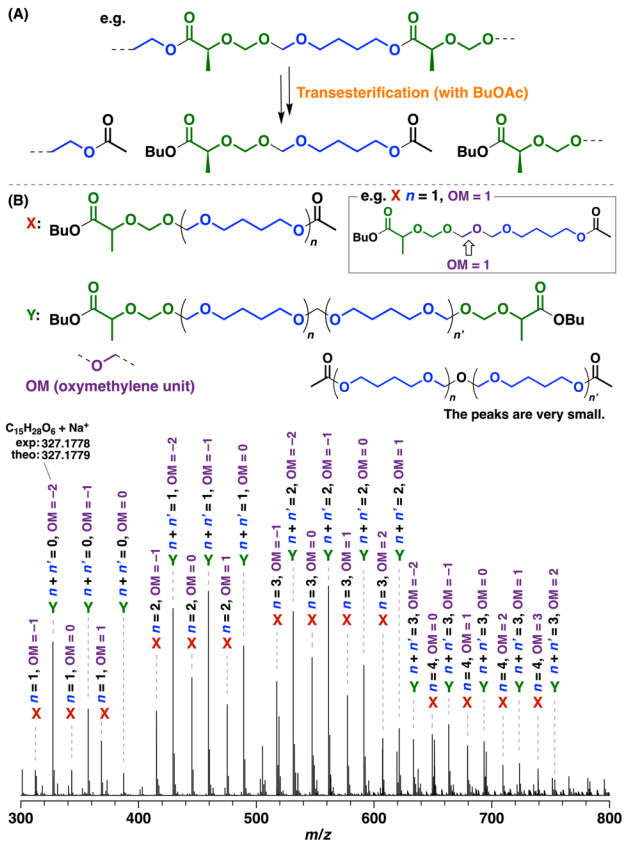

Figure 4. (A) An example of transesterification processes and (B) ESI-MS spectrum (recorded by equipment with the Kingdon trap) of the product obtained by transesterification of the DOP–**1** copolymer (the same sample as that shown in Figure 1C (orange curve); see Figure S4 for the ^{1}H NMR spectrum).

Transacetalization using 1,1-diethoxyethane by acid catalysis was also conducted to confirm the presence of formal units. A product with a very low MW (M_n = 0.2 × 10^3) was obtained after the reaction (Figure S5B). The ^{1}H NMR spectrum of the product exhibited peaks assignable to the structure resulting from transacetalization between 1,1-diethoxyethane and the formal moieties in the original copolymer (Figure S5A). The result indicates that the original copolymer contained many formal units in the main chain.

Plausible Copolymerization Mechanisms

Copolymers obtained by the copolymerization of DOP and **1** most likely contain DOP units, **1** units, and consecutive formal units, as demonstrated by the structural analyses. Plausible copolymerization mechanisms are proposed in this subsection. The crossover reaction from the DOP-derived propagating species to **1** and subsequent ring-opening do not occur (Scheme 3F), as confirmed by the absence of hemiformal units (vide supra),[31] unlike the cationic copolymerization of oxiranes and DOLOs (Scheme 1B). Therefore, **1** most likely reacts via the AM mechanism that involves the activation of **1** by a proton and subsequent reaction with a hydroxy group, resulting in a hemiformal (–O–CH_2–OH) end (Scheme 3A). Initiators such as alcohols were not used; hence, adventitious water most likely triggers the generation of a hydroxy group from monomers with the aid of the acid catalyst. Indeed, polymer chains with water-derived chain ends (one end derived from a proton of water or the acid catalyst (e.g. H–$OCH_2CH_2CH_2CH_2OCH_2$~~) and the other end derived from a hydroxy group of water (e.g. ~~$OCH_2CH_2CH_2CH_2OCH_2$–OH) were detected in the ESI-MS analysis (vide supra; Figure 3). The pathways that generate structures i–vi, as shown in Figure 2, are reasonably explained as follows: The hemiformal end reacts with the DOP-derived oxonium ion or a

proton-attached hemiformal end to generate structures i or ii, respectively (Scheme 3B). A DOP-derived hydroxy end also reacts with a proton-attached hemiformal end to generate structure iii (Scheme 3B). A hemiformal end also reacts with a midchain formal moiety via transacetalization reactions to afford structures i and iv, as shown in Scheme 3C. In addition, transacetalization reactions between midchain structures possibly occur to generate structures v and vi (Scheme 3D). Transacetalization reactions potentially occur at any formal moieties in polymer chains (Scheme S1), which results in diverse polymer structures composed of DOP, **1**, and formal units. Cyclic chains detected by the ESI-MS analysis (Figure 3) were generated when the reactions between chain ends (Scheme 3B), midchain moiety and chain end (Scheme 3C), or midchain moieties (Scheme 3D) occurred in a single chain. During the copolymerization, DOP homosequences are generated (Scheme 3E), while **1** does not undergo homopropagation, as suggested by the absence of peaks assignable to **1** homosequences and the inertness of **1** in homopolymerization under the same conditions (entry 10 in Table 1). ^{1}H NMR analysis during the copolymerization in CD_2Cl_2 (Figure S6) indicated that DOP homosequences were preferentially generated (Scheme 3E) at the early stage, while **1** was gradually consumed by the mechanism explained above. The generation of DOP homosequences could be reduced in the copolymerization reaction at a higher concentration of **1** compared to that of DOP (entry 9 in Table 1; Figure 1E).

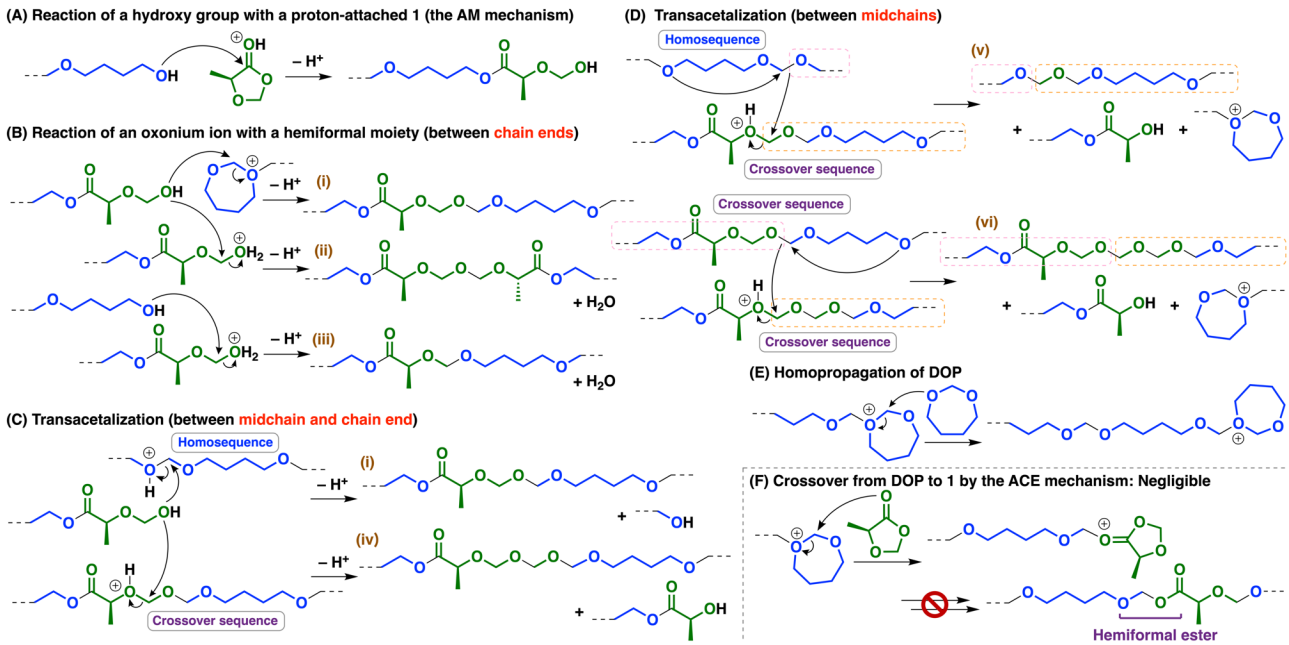

Scheme 3. Representative Examples of Reactions That Occur in the Copolymerization of DOP and **1**[a]

[a] Similar reactions occur among various chain ends and midchain acetal structures. See also Scheme S1.

The reaction of **1** by the AM mechanism was confirmed by a model reaction using an alcohol as a substrate. When **1** and 1-hexanol were reacted with CF_3SO_3H as a catalyst, compounds consisting of **1**-derived units and two hexyloxy groups (compounds I–IV) were produced, as confirmed by ^1H NMR and ESI-MS analyses (Figure 5). These compounds were most likely generated by the reaction of a proton-activated **1** and 1-hexanol and subsequent transacetalization reactions (Figure 5) in a manner similar to the reactions shown in Scheme 3.

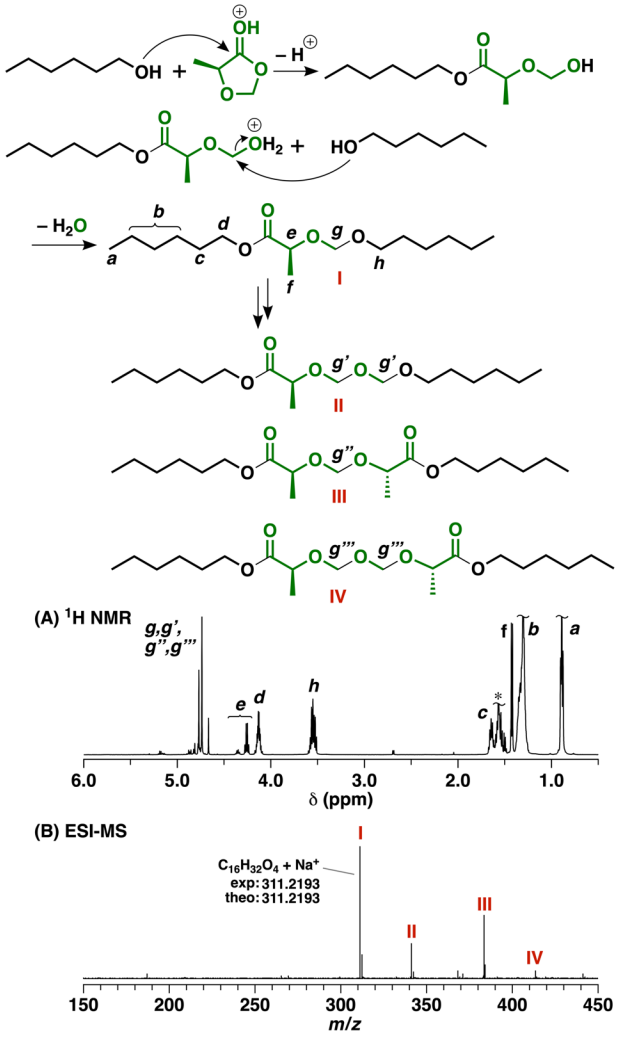

Figure 5. A model reaction of **1** and 1-hexanol. (A) ^{1}H NMR and (B) ESI-MS spectra of the product ([**1**]$_0$ = 0.10 M, [1-hexanol]$_0$ = 0.10 M, [CF_3SO_3H]$_0$ = 4.0 mM, in dichloromethane at 30 ºC; * water). Other products than I–IV may also be included.

Cationic Copolymerization of Other Cyclic Acetals and DOLOs

Cyclic acetals exhibit different reactivities depending on the number of ring members; hence, 1,3-dioxane (DOX) and 1,3-dioxolane (DOL), which have six- and five-membered structures, respectively, were copolymerized with **1**. 1,3,6-Trioxocane (TOC), which has an eight-membered ring with an additional oxygen atom, was also used. As a result, DOX was completely inert (entry 11 in Table 1), while copolymers were obtained from DOL and TOC (entries 12 and 13; Figure 1F and G). ^{1}H NMR analysis of the products suggested that copolymers were generated with consecutive formal units, as observed for the DOP–**1** copolymer (Figures S7 and S8). In the ESI-MS analysis of the DOL–**1** copolymer (Figure S9), peaks with *m*/*z* values corresponding to cyclic and linear chains

consisting of both DOL and **1** units were detected. However, the MW of the DOL–**1** copolymer was lower and the incorporated amount of **1** in the TOC–**1** copolymer was smaller compared to the DOP–**1** copolymer.

To examine the effects of DOLO structures, other DOLOs (Scheme 2) were used instead of **1** in the copolymerization with DOP. 2,5-Dimethyl-1,3-dioxolan-4-one (**2**) contains a methyl group at the 2-position, which severely affected the result (entry 2 in Table 2). A polymer was obtained from DOP and **2**; however, the MW was very small (M_n = 1.0 × 10^3). In the ^{1}H NMR spectrum of the product (Figure S10), the peak of the methyl group at the 2-position was obviously smaller than the peak of the methyl group at the 5-position. This result suggests that acetaldehyde was eliminated from a hemiacetal end produced by the reaction of a hydroxy group and a proton-activated **2** by the AM mechanism (Scheme 4). Elimination of acetaldehyde was reported in studies on polymerizations of DOLOs or six-membered cyclic hemiacetal esters.[24,32,33] Compared to the hemiformal end, the hemiacetal end is less stable,[34–36] which is probably responsible for acetaldehyde elimination.

Table 2. Cationic Copolymerizations of DOP and DOLOs[a]

entry	DOLO	time	conv. (%)		$M_n \times 10^{-3}$ [b]	M_w/M_n [b]	unit ratios[c]
			DOP	DOLO			DOP/DOLO
1	**1**	118 h	73	36	4.2 (15)[d]	5.96	2.1/1.0
2	**2**	75 h	56	43	1.0	2.78	1.3/1.0
3	**3**	92 h	79	17	3.0 (9.5)[d]	5.43	4.7/1.0
4	**4**	73 h	59	<1	2.4 (15.9)[d]	9.33	–

[a] $[DOP]_0$ = 1.5 (entries 1, 3, and 4) or 3.0 (entry 2) M, $[DOLO]_0$ = 1.5 (entries 1, 3 and 4) or 3.0 (entry 2) M, $[CF_3SO_3H]_0$ = 4.0 mM, in dichloromethane at 25 (room temperature; entry 1) or 30 (entries 2–4) ºC. Entry 1 is the same data as entry 7 in Table 1. [b] By GPC (polystyrene calibration). [c] Calculated by ^{1}H NMR. [d] Values for a main peak.

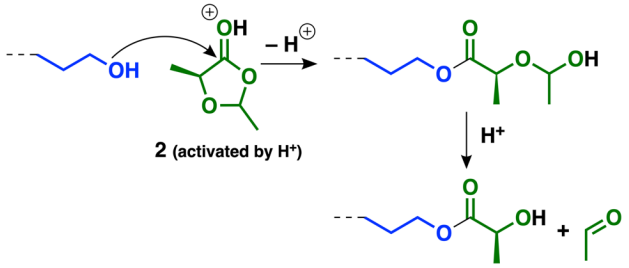

Scheme 4. Plausible Mechanism of the Copolymerization of **2** and DOP.

When 5-phenyl-1,3-dioxolan-4-one (**3**), which contains a phenyl group at the 5-position instead of a methyl group, was copolymerized with DOP, a copolymer with an M_n value of 3.0×10^3 was obtained (entry 3 in Table 2; Figure S11). The copolymer most likely exhibited a structure similar to that of the DOP–**1** copolymer (Figure 6), although the incorporated amount of **1** was smaller. Compared to **1**, the incorporation of **3** is less efficient, which likely results from the bulkiness of the phenyl group. The effect of the phenyl group was also supported by the result using 5,5-diphenyl-1,3-dioxolan-4-one (**4**), which contains two phenyl groups at the 5-position. Compound **4** was not consumed in the reaction with DOP, resulting in a DOP homopolymer (entry 4 in Table 2). The two phenyl groups likely disturbed the reactions with a hydroxy group by the AM mechanism.

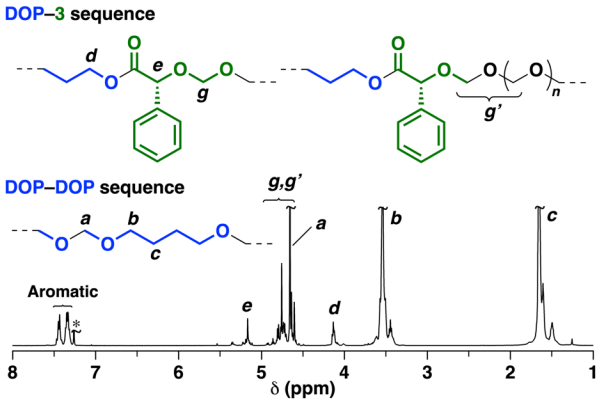

Figure 6. ^{1}H NMR spectrum of the DOP–**3** copolymer (entry 3 in Table 2; a high-MW portion separated by preparative GPC; in $CDCl_3$ at 30 ºC; * $CHCl_3$.)

DSC Analysis of Copolymers

The thermal properties of poly(DOP-*co*-**1**) and poly(DOP-*co*-**3**) were examined by differential scanning calorimetry (DSC) analysis (Table 3; after low-MW portions were removed by preparative GPC). The T_g of poly(DOP-*co*-**1**) was detected at –60 °C, which was higher than that of poly(DOP) (–78 °C[37]). In addition, poly(DOP-*co*-**3**) exhibited a higher T_g of –27 °C, likely due to the effect of the phenyl groups.

Table 3. T_g Values of Polymers[a]

polymer	$M_n \times 10^{-3}$ [b]	M_w/M_n [b]	unit ratios[c]		T_g (ºC)
			DOP	DOLO	
poly(DOP-*co*-**1**)	19.3	1.89	1.9	1.0	–60
poly(DOP-*co*-**3**)	13.3	1.78	1.5	1.0	–27
poly(DOP)	–	–	–	–	–78[d]

[a] By DSC (2nd heating scan, 10 ºC/min). DSC curves are summarized in Figure S12. [b] By GPC (polystyrene calibration). After low-MW portions were removed by preparative GPC. [c] Calculated by ^{1}H NMR. [d] From reference 37.

Conclusion

In conclusion, cationic copolymerizations of appropriate cyclic acetals and DOLOs successfully proceeded with a strong protic acid as a catalyst. The detailed analysis of the copolymer structures by NMR and ESI-MS revealed that the copolymers were generated via the AM mechanism. Transacetalization reactions also occurred during copolymerization, resulting in consecutive formal structures in polymer chains. In addition, the copolymers were degraded via the cleavage of ester and formal moieties by transesterification and transacetalization, respectively. The results obtained in this study contribute to the development of design strategies for cationic ring-opening copolymerizations of different types of cyclic monomers. We will further investigate the cationic copolymerizations of various pairs of monomers in future studies.

Associated Content

Supporting Information

Experimental section, polymerization data, and NMR spectra of polymerization products.

Corresponding Authors

E-mail: kanazawaa11@chem.sci.osaka-u.ac.jp (A.K); aoshima@chem.sci.osaka-u.ac.jp (S.A.)

Notes

The authors declare no competing financial interest.

Acknowledgments

This work was partially supported by JSPS KAKENHI Grants 18K05217 and 23H02010. We thank Dr. Naoya Inazumi (Osaka University) for the DOSY measurement.

References and Notes

1. Okada, M.; Takikawa, N.; Iwatsuki, S.; Yamashita, Y.; Ishii, Y. Cationic Copolymerization of 1,3-Dioxolane and Some Cyclic Ethers. *Makromol. Chem.* **1965**, *82*, 16–24.
2. Ito, K.; Inoue, T.; Yamashita, Y. Copolymerizations of 3.3-Bis(chloromethyl)oxacyclobutane with β-Propiolactone and γ-Butyrolactone by Lewis Acids: "Two-State" Polymerization Mechanism. *Makromol. Chem.* **1970**, *139*, 153–164.
3. Yamashita, Y.; Kondo, S.; Ito, K. Cationic Copolymerization of b,b-Dimethyl-b-propiolactone with 1,3-Dioxolane, 3,3-Bis(chloromethyl)oxacyclobutane and Styrene. High-Resolution NMR Studies on Sequence Distribution of Copolymers. *Polym. J.* **1970**, *1*, 327–333.
4. Yamashita, Y.; Ito, K.; Chiba, K.; Kozawa, S. Cationic Copolymerization of Tetrahydrofuran with ε-Caprolactone. *Polym. J.* **1971**, *3*, 389–393.
5. Sudo, A.; Suzuki, A.; Endo, T. Cationic Copolymerization Behavior of Epoxide and 3-Isochromanone. *J. Polym. Sci., Part A: Polym. Chem.* **2013**, *51*, 4213–4220.
6. Bednarek, M.; Basko, M.; Kubisa, P. Functional Polylactide by Cationic Ring-Opening Copolymerization of Lactide with Epoxides. *React. Func. Polym.* **2017**, *119*, 9–19.
7. Le Bellec, P.; Midoux, P.; Cheradame, H.; Bennevault, V.; Guégan, P. Tuneable Thermal Properties of PTHF-Based Copolymers by Incorporation of Epoxide Units. *Eur. Polym. J.* **2022**, *168*, 111096.
8. Zhang, X.; Zhang, C.; Zhang, X. A Facile and Unprecedented Route to a Library of Thermostable Formaldehyde-Derived Polyesters: Highly Active and Selective Copolymerization of Cyclic Acetals and Anhydrides. *Angew. Chem. Int. Ed.* **2022**, *61*, e202117316.
9. Dirauf, M.; Muljajew, I.; Weber, C.; Schubert, U. S. Recent Advances in Degradable Synthetic Polymers for Biomedical Applications – Beyond Polyester. *Prog. Polym. Sci.* **2022**, *129*, 101547.
10. Wang, X.; Huo, Z.; Xie, X.; Shanaiah, N.; Tong, R. Recent Advanced in Sequence-Controlled Ring-Opening Copolymerizations of Monomers Mixtures. *Chem. Asian J.* **2023**, *18*, e202201147.
11. Kubisa, P. In *Polymer Science: A Comprehensive Reference*; Matyjaszewski, K., Möller, M., Eds.; Elsevier B.V.: Amsterdam, 2012; Vol. *4.08*.
12. Kubisa, P.; Vairon, J. P. In *Polymer Science: A Comprehensive Reference*; Matyjaszewski, K., Möller, M., Eds.; Elsevier B.V.: Amsterdam, 2012; Vol. *4.10*.
13. Okamoto, Y. Cationic Ring-Opening Polymerization of Lactones in the Presence of Alcohol. *Makromol. Chem., Macromol. Symp.* **1991**, *42/43*, 117–133.
14. Kubisa, P.; Penczek, S. Cationic Activated Monomer Polymerization of Heterocyclic Monomers. *Prog. Polym. Sci.* **1999**, *24*, 1409–1437.
15. Endo, T.; Shibasaki, Y.; Sanda, F. Controlled Ring-Opening Polymerization of Cyclic Carbonates and Lactones by an Activated Monomer Mechanism. *J. Polym. Sci., Part A: Polym. Chem.* **2002**, *40*, 2190–2198.
16. Penczek, S.; Pretula, J. Activated Monomer Mechanism (AMM) in Cationic Ring-Opening Polymerization. The Origin of the AMM and Further Development in Polymerization of Cyclic Esters. *ACS Macro Lett*. **2021**, *10*, 1377−1397.
17. Higuchi, M.; Kanazawa, A.; Aoshima, S. Tandem Unzipping and Scrambling Reactions for the Synthesis of Alternating Copolymers by the Cationic Ring-Opening Copolymerization of a Cyclic Acetal and a Cyclic Ester. *ACS Macro Lett.* **2020**, *9*, 77–83.
18. Higuchi, M.; Kanazawa, A.; Aoshima, S. Unzipping and Scrambling Reaction-Induced Sequence Control of Copolymer Chains via Temperature Changes during Cationic Ring-Opening Copolymerization of Cyclic Acetals and Cyclic Esters. *J. Polym. Sci.* **2021**, *59*, 2730–2741.
19. Kost, B.; Basko, M. Synthesis and Properties of L-Lactide/1,3-Dioxolane Copolymers: Preparation of Polyesters with Enhanced Acid Sensitivity. *Polym. Chem.* **2021**, *12*, 2551–2562.

20. Hyoi, K.; Kanazawa, A.; Aoshima, S. Cationic Ring-Opening Co- and Terpolymerizations of Lactic Acid-Derived 1,3-Dioxolan-4-ones with Oxiranes and Vinyl Ethers: Nonhomopolymerizable Monomer for Degradable Co- and Terpolymers. *ACS Macro Lett.* **2019**, *8*, 128–133.
21. Ôeda, H. Acetone-Compounds of Some α-Hydroxy-Acids and Their Raman Spectra. *Bull. Chem. Soc. Jpn.* **1935**, *10*, 187–192.
22. Polonski, T. Optical Activity of Lactones and Lactams–I. Conformational Dependence of the Circular Dichroism of 1,3-Dioxolan-4-ones. *Tetrahedron* **1983**, *39*, 3131–3137.
23. Martin, R. T.; Camargo, L. P.; Miller, S. A. Marine-Degradable Polylactic Acid. *Green Chem.* **2014**, *16*, 1768–1773.
24. Cairns, S. A.; Schultheiss, A.; Shaver, M. P. A Broad Scope of Aliphatic Polyesters Prepared by Elimination of Small Molecules from Sustainable 1,3-Dioxolan-4-ones. *Polym. Chem.* **2017**, *8*, 2990–2996.
25. Neitzel, A. E.; Haversang, T. J.; Hillmyer, M. A. Organocatalytic Cationic Ring-Opening Polymerization of a Cyclic Hemiacetal Ester. *Ind. Eng. Chem. Res.* **2016**, *55*, 11747–11755.
26. Neitzel, A. E.; Barreda, L.; Trotta, J. T.; Fahnhorst, G. W.; Haversang, T. J.; Hoye, T. R.; Fors, B. P.; Hillmyer, M. A. Hydrolytically-Degradable Homo- and Copolymers of a Strained Exocyclic Hemiacetal Ester. *Polym. Chem.* **2019**, *10*, 4573–4583.
27. Okada, M.; Sumitomo, H.; Yamamoto, Y. Cationic Polymerization of 6,8-Dioxabicyclo[3.2.1]octan-7-one. *Makromol. Chem.* **1974**, *175*, 3023–3028.
28. Morris, K. F.; Johnson, C. S. Resolution of Discrete and Continuous Molecular Size Distributions by Means of Diffusion-Ordered 2D NMR Spectroscopy. *J. Am. Chem. Soc.* **1993**, *115*, 4291–4299.
29. Groves, P. Diffusion Ordered Spectroscopy (DOSY) as Applied to Polymers. *Polym. Chem.* **2017**, *8*, 6700–6708.
30. Peter, A.; Fehr, S. M.; Dybbert, V.; Himmei, D.; Lindner, I.; Jacob, E.; Ouda, M.; Shaadt, A.; White, R. J.; Scherer, H.; Krosing, I. Towards a Sustainable Synthesis of Oxymethylene Dimethyl Ether by Homogeneous Catalysis and Uptake of Molecular Formaldehyde. *Angew. Chem. Int. Ed.* **2018**, *57*, 9461–9464.
31. There is a possibility that hemiacetal ester moieties were generated via the reaction shown in Scheme 3F and subsequently consumed by acid-catalyzed interchain reactions in a manner similar to transacetalization reactions. In addition, very small peaks (the integral ratios were approximately 1% of those of peaks *a*, *h*, *h′*, and *h″*), which are likely assigned to hemiacetal ester moieties, were observed at 5.2–5.5 ppm in the spectrum in Figure 2A.
32. Neitzel, A. E.; Peterson, M. A.; Kokkoli, E.; Hillmyer, M. A. Divergent Mechanistic Avenues to an Aliphatic Polyesteracetal or Polyester from a Single Cyclic Esteracetal. *ACS Macro Lett.* **2014**, *3*, 1156–1160.
33. Kohsaka, Y.; Yamashita, M.; Matsuhashi, Y.; Yamashita, S. Synthesis of Poly(Conjugated Ester)s by Ring-Opening Polymerization of Cyclic Hemiacetal Ester Bearing Acryl Skeleton. *Eur. Polym. J.* **2019**, *120*, 109185.
34. We think that hemiformals are more stable than hemiacetals because formals show less reactivity in acid hydrolysis than acetals (reference 35) and a hydrate of formaldehyde is more preferentially generated in water than a hydrate of acetaldehyde (reference 36).
35. Satchell, D. P. N.; Satchell, R. S. Mechanisms of Hydrolysis of Thioacetals. *Chem. Soc. Rev.* **1990**, *19*, 55–81.
36. Bell, R. P. The Reversible Hydration of Carbonyl Compounds. *Adv. Phys. Org. Chem.* **1966**, *4*, 1–29.
37. Vuluga, D.-M.; Pantiru, M.; Hamaide, T.; Vasilescu, D. S. Study of Dioxolane-Dioxepane Copolymers through IR and DSC. *Polym. Bull.* **2004**, *52*, 349–354.